Engineering Structures 262 (2022) 114326

Contents lists available at ScienceDirect

Engineering Structures

journal homepage: www.elsevier.com/locate/engstruct

# Dynamic impact of automated truck platooning on highway bridges

Tianyang Ling [a], Ran Cao [a], Lu Deng [a,b,*], Wei He [a], Xin Wu [c], Wenjie Zhong [d]

[a] *College of Civil Engineering, Hunan University, Changsha, 410082, China*
[b] *Hunan Provincial Key Laboratory for Damage Diagnosis of Engineering Structures, Hunan University, Changsha, 410082, China*
[c] *Hunan Communication Research Institute Co., Ltd., Changsha, 410200, China*
[d] *Computational Marine Hydrodynamics Lab (CMHL), School of Naval Architecture, Ocean and Civil Engineering, Shanghai Jiao Tong University, Shanghai, 200240, China*

ARTICLE INFO

*Keywords:*
Highway bridge
Automated truck platooning
Bridge resonance
Dynamic load allowance

ABSTRACT

Automated truck platooning (ATP) has attracted growing attention since it can significantly promote energy conservation and increase transport efficiency by arranging moving trucks at close distances. Currently, the ATP has been widely implemented, but its effects on bridges have not been considered in the original design of many existing highway bridges. Hence, these bridges may not be capable of sustaining the load of ATP. Some assessments have been conducted, but little attention has been paid to the ATP-induced dynamic impact, which is more critical to the design and evaluation of a bridge. In this paper, this problem was investigated using both theoretical analysis and numerical simulation. The theoretical derivation was conducted to investigate the ATP-induced bridge vibration, particularly in resonance conditions. It was found that typical highway bridges could be at a high risk of resonance induced by the ATP moving at normal speeds. For more comprehensive assessments, numerical simulations were performed based on a refined vehicle-bridge interaction (VBI) simulation system, and the effect of critical parameters were studied, including vehicle speed, inter-truck spacing and so forth. Results show that the dynamic impact on the bridge induced by ATP can be significantly larger than that caused by a single truck due to the superposition effect. Such effect is caused by the combination of speed and inter-truck spacing, it can also be greatly affected by the number of trucks and road surface conditions. The simulation results also show that the current code-specified dynamic load allowance (DLA), particularly for the Chinese code and Eurocode, may not be sufficiently capable of characterizing the dynamic effects of ATP loads. Accordingly, a strategy of arranging ATP crossing highway bridges was proposed to reduce the adverse dynamic impact.

## 1. Introduction

Automated truck platooning (ATP) is an important future-oriented transport strategy, which helps manage multiple rapidly moving trucks at close distances to reduce the aerodynamic drag [1]. Promoted by the rapidly advancing 5th generation mobile network (5G) and vehicle-to-vehicle (V2V) communication technology, the ATP has attracted increasing attention from both research and industry [1–4] due to its evidence-based promotion of fuel savings [1], emission reductions [3], and many other benefits [2,5,6].

Deployment of ATP significantly increases the probability of multiple closely spaced (<15 m) heavy trucks running in the same lane [7], for which current physical infrastructures, particularly pavements and bridges, may suffer negative impacts. However, such incident has almost not been considered in the design method of infrastructure systems in many countries [5,8].

Recent studies [9–12] have shown that reducing the wandering of ATP accelerates pavement damage and shortens pavement life. To address this problem, controlled lane positioning technology [9–11] was proposed, and it has little influence on the energy efficiency of ATP [12]. Compared to pavements, bridge structures are more susceptible to closely spaced vehicular loads, which could occur for ATP due to the short time delay (0.3–0.5 s) [2] of the V2V communication. Some research has been carried out to evaluate the loading effect of ATP on bridges. DeVault et al. [13] defined a load rating factor (ratio of the live load effect generated by ATP to the standard live load effect) to assess the load effect of ATP. It was found that some specific bridge structures in Florida state cannot sustain the load of a two-truck platoon.

* Corresponding author.
*E-mail address:* denglu@hnu.edu.cn (L. Deng).

https://doi.org/10.1016/j.engstruct.2022.114326
Received 12 October 2021; Received in revised form 1 April 2022; Accepted 24 April 2022
Available online 18 May 2022

Kamranian et al. [14] focused on the Hay River bridge and obtained similar conclusions. Besides, it was revealed that ATP threatens not only the superstructures but also the substructures of the bridge [8] due to the transfer of the increased internal forces, including bending moment, shear force, and support reaction. As for steel bridges, the long-term fatigue damage was also affected by the ATP [15], and the platoon gap is a critical parameter. Birgisson et al. [3] pointed out that reducing the platoon gap may result in greater bridge-loading capacity demand, which is uneconomical. The report [3] from the Department of Transportation in Texas indicated that traditional bridge design methods might not be capable of accommodating the emerging truck platoons. Thus, the current live load design method of the bridge may need to be modified to handle the load of truck platooning [16,17].

Most of the aforementioned assessments were carried out based on the static analysis method and more focused on the added static effect [16]. In fact, the impacts of ATP on the bridge structures are not limited to the increase in static loads, since closely spaced trucks usually move at high speeds [18] and dynamically interact with the bridges [19]. Although the interaction between multiple vehicles and bridges has been studied [20,21], little attention has been paid to closely spaced heavy-duty trucks involved in ATP. Furthermore, similar to the train loading [22], when the loading frequency formed by multi-vehicles approaches the natural frequencies of the bridge, resonance might be excited and cause significant bridge dynamic responses, even collapses [23]. Therefore, it is of great urgency and necessity to conduct an in-depth analysis of the ATP-bridge interaction problem to address the potential adverse impacts.

In this study, theoretical analysis of the bridge vibration under ATP-load is firstly carried out based on a simplified model (in Section 2) to investigate the general rules of bridge resonance induced by ATP. To explore the problem in a more realistic scenario, a series of numerical simulations is then conducted (in Section 4) based on a refined vehicle-bridge interaction (VBI) simulation system (introduced in Section 3), in which several critical factors (i.e., truck speed, inter-truck spacing, truck platoon size, and road surface conditions) are considered. For every simulation scenario, the dynamic load allowance (DLA) of the bridge is calculated to quantify the dynamic impact caused by the ATP. It is found that under some loading conditions, the bridge response is significantly increased due to resonance, and therefore the code-specified DLAs of the bridge can be exceeded by a large extent. Moreover, the negative impact can be further aggravated by the truck platoon size and road surface conditions. A traffic strategy is proposed (in Section 5) to reduce the potential adverse impacts of ATP on highway bridges.

## 2. Bridge resonance under moving truck platoon-loads

### 2.1. Truck platoon-bridge model

The vibration of a bridge is inevitable to be excited by moving vehicles, particularly by a series of heavy trucks. Considering the mass ratio of a truck to highway bridge is generally smaller than 1, the additional mass of the vehicle has little influence on the effective frequency of the bridge-vehicle system [24]. Thus, the truck platoon-bridge system can be simplified as an Euler–Bernoulli beam under a load of a series of concentrated forces ($P$), spaced by the critical wheelbase ($l_c$), and inter-truck spacing ($d_v$), as shown in Fig. 1.

To further simplify the analysis, the truck platoon composed of $n$ closely spaced (<15 m) trucks can be ideally described as $2n$ moving forces with constant spacing ($d_v$). Assuming the position of the front axle of the lead truck is $x$, which can be determined by the truck speed $v$ and time $t$, the time interval ($\Delta t$) required for the latter force to arrive can be calculated by $d_v/v$. Thus, the motion equation of the simply supported beam without damping can be expressed as [22]

$$EI\frac{\partial^4 y(x,t)}{\partial x^4}+\overline{m}\frac{\partial^2 y(x,t)}{\partial t^2}=\sum_{k=0}^{2n-1}\delta\left[x-v\left(t-\frac{k\cdot d_v}{v}\right)\right]P \tag{1}$$

where $\overline{m}$ and $I$ are the constant mass and constant moment of inertia of the bridge cross-section, respectively; $E$ is the elastic modulus of the materials used in bridge structure; $y(x,t)$ is the displacement of the bridge at position $x$ and time $t$; $\delta$ is the Dirac function.

### 2.2. Analytical solution for bridge response

To solve Eq. (1), a partial differential equation, the modal decomposition method is adopted to express the bridge displacement in generalized coordinates $q(t)$ and mode shapes. Hence, Eq. (1) can be rewritten as

$$\ddot{q}_i(t)+\omega_i^2 q_i(t)=\frac{2P}{\overline{m}L}\sum_{k=0}^{2n-1}\sin\frac{i\pi v}{L}\left(t-\frac{k\cdot d_v}{v}\right) \tag{2}$$

where $L$ is the bridge span length; $\omega_j = (j\pi^2/L^2)\sqrt{EI/\overline{m}}$ is the $j$th circular frequency of the bridge. If only consider the first vibration mode of the bridge, i.e., $\omega = (\pi^2/L^2)\sqrt{EI/\overline{m}}$, the general solution of Eq. (1) can be obtained as

$$q(t)=\frac{2PL^3}{EI\pi^4}\cdot\frac{1}{1-\beta^2}\sum_{k=0}^{2n-1}\left[\sin\overline{\omega}\left(t-\frac{k\cdot d_v}{v}\right)-\beta\sin\omega\left(t-\frac{k\cdot d_v}{v}\right)\right] \tag{3}$$

where $\overline{\omega}=\pi v/L$ is the exciting frequency of the moving axle loads of the truck platoon; $\beta=\overline{\omega}/\omega$ is the ratio of the exciting frequency to the fundamental frequency of the bridge, and the dynamic amplification factor can be calculated by $1/(1-\beta^2)$. Thus, the dynamic displacement response of the bridge can be expressed as

$$y(x,t)=\frac{2PL^3}{EI\pi^4}\cdot\frac{1}{1-\beta^2}\sin\frac{\pi x}{L}\cdot\left[\sum_{k=0}^{2n-1}\sin\overline{\omega}\left(t-\frac{k\cdot d_v}{v}\right)-\beta\sum_{k=0}^{2n-1}\sin\omega\left(t-\frac{k\cdot d_v}{v}\right)\right] \tag{4}$$

On the right side of Eq. (4), the first term represents the forced response of the beam induced by the moving axle loads, while the second term is associated with free vibration due to the former forces that have left the bridge. These two types of responses were termed steady and transient responses [25], respectively, because of different mechanisms.

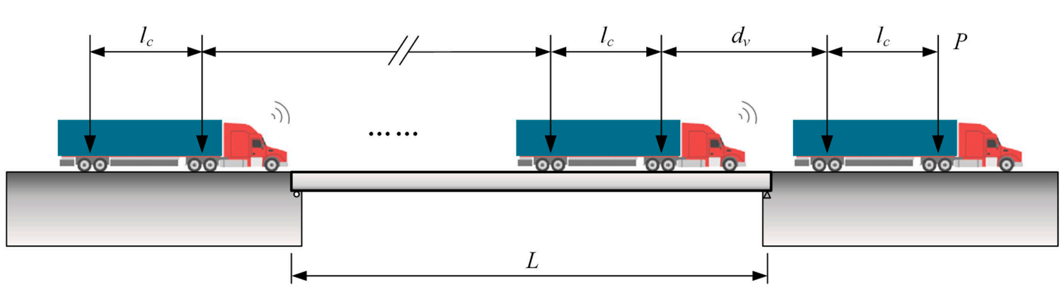


**Fig. 1.** Simply supported bridge under the load of truck platooning.

### 2.3. Bridge resonance induced by periodical truck platoon loads

The transient response of Eq. (4) can be rewritten into the following form after adopting the transformation of triangular progression.

$$\sum_{k=0}^{2n-1}\sin\omega\left(t-\frac{k\cdot d_v}{v}\right) = \sin\omega t + \sum_{k=1}^{2n-1}\sin\omega\left(t-\frac{k\cdot d_v}{v}\right)$$
$$= \sin\omega t + \frac{\sin\left[(2n-1)\cdot\frac{\omega d_v}{2v}\right]\cdot\sin\left[\omega t-2n\cdot\frac{\omega d_v}{2v}\right]}{\sin\frac{\omega d_v}{2v}} \quad (5)$$

When applying L'Hospital's rule, the limit solution of the equation above can be expressed as

$$\lim_{\frac{\omega d_v}{2v}\to\pm i\pi}\frac{\sin\left[(2n-1)\cdot\frac{\omega d_v}{2v}\right]\cdot\sin\left[\omega t-2n\cdot\frac{\omega d_v}{2v}\right]}{\sin\frac{\omega d_v}{2v}} = (2n-1)\sin\omega\left(t-n\cdot\frac{d_v}{v}\right) \quad (6)$$

Considering the physical significance, the extreme condition for Eq. (6) is

$$\frac{\omega\cdot d_v}{2v} = i\pi \qquad (i = 1,\ 2,\ 3\ldots) \quad (7)$$

Substituting this extreme condition into Eq. (5), the limit value of the transient response in Eq. (4) is obtained as

$$\sum_{k=0}^{2n-1}\sin\omega\left(t-\frac{k\cdot d_v}{v}\right)\Big|_{\frac{\omega d_v}{2v}=i\pi} = 2n\sin\omega t \quad (8)$$

According to Eq. (8), it can be deduced that the transient response can be excited by every axle force in a truck platoon, and the amplitude of the response will be repeatedly enlarged with the increase in the number of trucks $n$ of the platoon. Similar results can be obtained when considering the higher modes of the bridge, so the resonance speed regarding the transient response of a bridge with the fundamental frequency of $f_{bj} = \omega_j/2\pi$ can be derived as

$$V_{br} = \frac{3.6\cdot f_{bj}\cdot d_v}{i}\,(j = 1,2,3\ldots;\ i = 1,2,3\ldots) \quad (9)$$

in which, $V_{br}$ is the resonance speed (km/h); $f_{bj}$ is the $j$th vertical fundamental frequency of the bridge (Hz), $d_v$ is the axle spacing of the truck platooning (m), and the multiplier $i = 1, 2, \ldots$ is determined by the extreme condition in Eq. (7).

According to Eq. (9), it can be observed that when the regularly arranged ($d_v$) ATP crosses the bridge at a resonance speed ($V_{br}$), different bridge resonance conditions can be satisfied for different multipliers $i$. Furthermore, multiple modal shapes of the bridge also correspond to different resonance conditions. Therefore, a series of bridge resonances may be induced under a load of ATP moving at random speeds.

Since the corresponding resonance speed of the steady response of a bridge is much higher than the truck operation speeds [25], the resonance condition of the steady response in Eq. (4) is not discussed here.

### 2.4. Problem statement

It is given that the cross-section stiffness of the bridge $EI = 1.66\times10^8$ kN·m$^2$, the mass constant $\overline{m} = 19.1$ t/m$^2$ [25], and these parameters are not changed along bridge span length. Taking both $j$ and $i$ as 1, all the resonance speeds for different combinations of axle spacing ($d_v$) and bridge span length (fundamental frequency) can be estimated by Eq. (9), as listed in Table 1. These speeds were also marked in Fig. 2(a) to compare with the operating speeds. Based on the data shown in Table 1 and Fig. 2, major observations were as follows:

(1) The resonance speed for a highway bridge can be lower than 100 km/h when the axle spacing of ATP ranges between 2 and 15 m [16]. The bridge with a lower fundamental frequency corresponds to a lower resonance speed, providing a low threshold for ATP.
(2) The normal truck operation speeds (60–100 km/h) have a significant overlap with the potential resonance speeds predicted for the highway bridges, whose fundamental frequencies ranged from 1.6 to 6.5 Hz (see in Fig. 2(a)). ATP-induced bridge resonance could occur for these bridges.
(3) Some other typical short-and medium-span bridges designed per current specifications [26,27] are also among the special bridges described in (2), as shown in Fig. 2(b) [28–30]. It should be noted that those bridges also include highway bridges with similar frequency characteristics (<6.5 Hz), including long-span bridges.

To sum up, a variety of highway bridges may be threatened by the ATP-induced resonance if the ATP were fully implemented. Similar problems [22] in railway bridges had been prevented by designing the bridge span to fixed lengths, but this "one size fits all" approach does not apply to highway bridges. Because a highway bridge is usually constructed according to the site condition, the platooning trucks moving on it also have various axle configurations and changeable spacings. Generally, the bridge with a lower fundamental frequency is prone to resonance excited by ATP moving at normal speeds. Meanwhile, the fundamental frequency of the bridge may also coincide with the low-natural frequencies of the truck [28], leading to bridge-vehicle resonance. All these mixed resonance conditions combined with the amplified effect of speed and road roughness could lead to a complicated ATP-bridge interaction problem, which entailed a more refined simulation system.

**Table 1**
Resonance speeds (km/h) for different combinations of fundamental frequency of the bridge and axle spacing of the trucks.

| $L_c$ (m) | Natural frequency (Hz) | | | | | | | | |
|---|---|---|---|---|---|---|---|---|---|
| | 40.52 | 18.01 | 10.13 | 6.48 | 4.50 | 3.31 | 2.53 | 2.00 | 1.65 |
| 2 | — | — | 72.94 | 46.68 | 32.42 | 23.82 | 18.23 | 14.41 | 11.67 |
| 3 | — | — | 109.41 | 70.02 | 48.62 | 35.72 | 27.35 | 21.61 | 17.50 |
| 4 | — | — | — | 93.36 | 64.83 | 47.63 | 36.47 | 28.81 | 23.34 |
| 5 | — | — | — | 116.70 | 81.04 | 59.54 | 45.59 | 36.02 | 29.17 |
| 6 | — | — | — | — | 97.25 | 71.45 | 54.70 | 43.22 | 35.01 |
| 7 | — | — | — | — | 113.46 | 83.36 | 63.82 | 50.43 | 40.84 |
| 8 | — | — | — | — | — | 95.26 | 72.94 | 57.63 | 46.68 |
| 9 | — | — | — | — | — | 107.17 | 82.05 | 64.83 | 52.51 |
| 10 | — | — | — | — | — | 119.08 | 91.17 | 72.04 | 58.35 |
| 11 | — | — | — | — | — | — | 100.29 | 79.24 | 64.18 |
| 12 | — | — | — | — | — | — | 109.41 | 86.44 | 70.02 |
| 13 | — | — | — | — | — | — | 118.52 | 93.65 | 75.85 |
| 14 | — | — | — | — | — | — | — | 100.85 | 81.69 |
| 15 | — | — | — | — | — | — | — | 108.05 | 87.52 |

Note: "—" represents resonance speeds greater than 120 km/h.

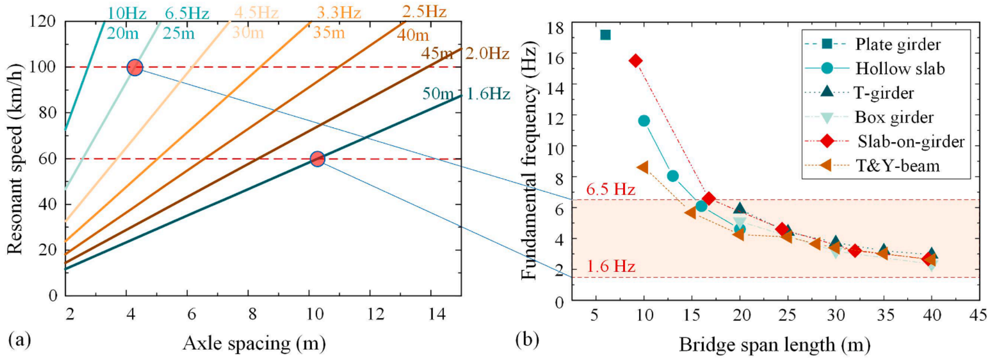


**Fig. 2.** Identification of bridge resonance: (a) identified resonance speed for different combinations of bridge fundamental frequency and axle spacing of the trucks; (b) fundamental frequencies for some typical short- and medium-span bridges.

## 3. Truck platoon-bridge interaction simulation system

The actual truck platoon-bridge interaction system is a complex three-dimensional system, in which the bridge response is greatly affected by the damping and stiffness of the vehicle and bridge [28]. Numerical simulation is an efficient method to analyze vehicle-bridge interaction (VBI) problems [22,28,31–33]. In this section, a refined VBI simulation system is developed to obtain more realistic bridge responses [34]. The accuracy of the developed VBI simulation system was verified in the previous studies [28,32], in which the simulated bridge responses, including strains and displacements, agreed very well with the real bridge responses measured in the field test.

### 3.1. Truck platoon model

Given that five-axle semi-trailer trucks are frequently used for platooning transport [16,17] due to their great cargo capacity, three five-axle semi-trailers (i.e., Chinese 5-axle truck [35], Florida C5 truck [17], and European 5-axle truck [36]) were considered in this study, as shown in Fig. 3(a). The analytical truck models (Fig. 3(b)) of the three trucks were developed according to the parameters listed in Table 2 [35,36]. The parameters of the Florida C5 truck model, except for the dimensions and weights, were taken the same as those of the other two truck models.

Platooning gap is a critical parameter in managing an automated truck platoon, and it usually represents the truck-to-truck distance [16]. For load effect analysis, however, it would be more reasonable to use the inter-truck spacing (axle-to-axle distance) to describe the relative distance, as shown in Fig. 4.

### 3.2. Bridge model

A simply-supported T-girder bridge was considered in this study. The bridge is a common type of highway bridge in China with structural characteristics similar to those of the slab-on-girder highway bridges designed per AASHTO-LRFD specifications [27]. Since the bridge with a longer span length (lower fundamental frequency) is prone to ATP-induced bridge resonance, the span length of the T-girder bridge was taken as 40 m. The corresponding dimensions of the cross-sectional (see Fig. 5(b)) can be determined according to standard drawings [37]. On this basis, the finite element model of the bridge was built in ANSYS using solid element SOLID185, as shown in Fig. 5(c). Rayleigh damping is used to represent the bridge damping effect, and the damping ratio is taken as 0.02, as adopted in other studies for similar bridges [38,39]. In order to achieve a good accuracy of the simulation while maintaining acceptable computation efficiency, the first 50 mode shapes of the

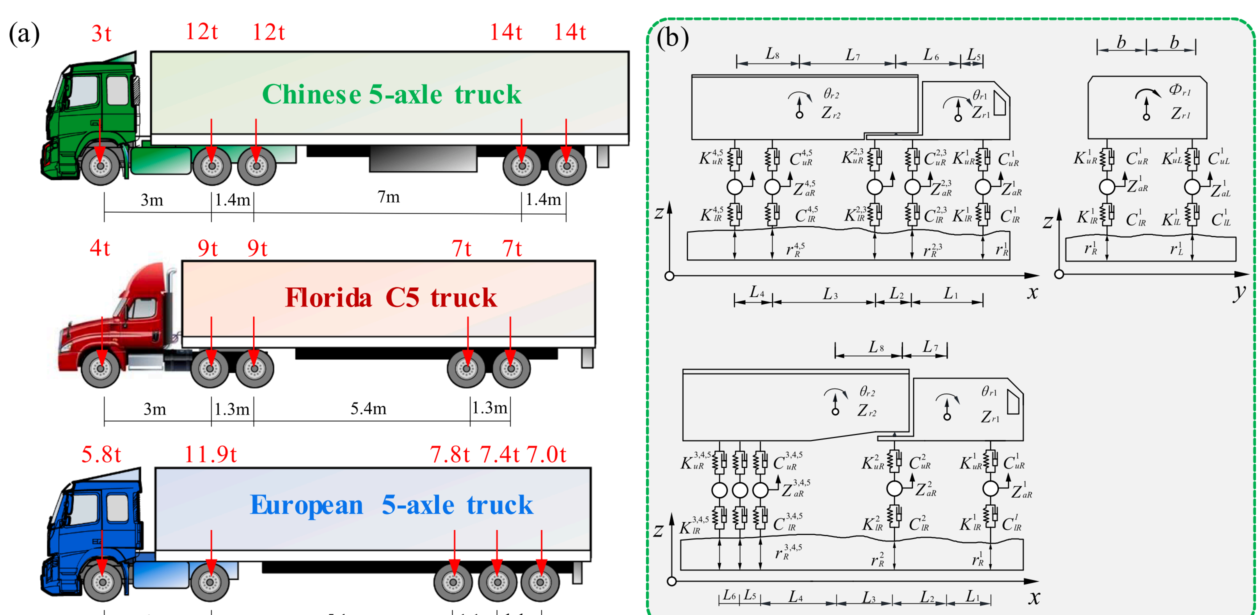


**Fig. 3.** Configurations of three typical trucks: (a) axle weights and spacings; (b) analytical truck models (refined tire model unassembled).

**Table 2**
Major parameters of the truck models in this study.

| Major parameters | | Unit | Chinese 5-axle truck [35] | Florida C5 truck | European 5-axle truck [36] |
|---|---|---|---|---|---|
| Gross mass of truck | | kg | 55,000 | 36,000 | 40,000 |
| Mass of truck body1 | | kg | 2,277 | 2,106 | 4,500 |
| Mass of truck body2 | | kg | 45,264 | 26,574 | 31,450 |
| Rolling moment of inertia of tuck body1 | | kg·m$^2$ | 20,196 | 20,196 | 460 |
| Rolling moment of inertia of tuck body2 | | kg·m$^2$ | 285,990 | 285,990 | 4,604 |
| Pitching moment of inertia of truck body1 | | kg·m$^2$ | 2,189.2 | 2,189.2 | 1,630 |
| Pitching moment of inertia of truck body2 | | kg·m$^2$ | 43,512 | 43,512 | 16,302 |
| Suspension mass | Axle-1 | kg | 700 | 700 | 700 |
| | Axle-2 | kg | 1,000 | 1000 | 1100 |
| | Axle-3 | kg | 1,000 | 1000 | 750 |
| | Axle-4 | kg | 800 | 800 | 750 |
| | Axle-5 | kg | 800 | 800 | 750 |
| Suspension stiffness coefficient | Axle-1 | N/m | 300,000 | 300,000 | 400,000 |
| | Axle-2 | N/m | 500,000 | 500,000 | 1000,000 |
| | Axle-3 | N/m | 500,000 | 500,000 | 750,000 |
| | Axle-4 | N/m | 400,000 | 400,000 | 750,000 |
| | Axle-5 | N/m | 400,000 | 400,000 | 750,000 |
| Suspension damping coefficient | Axle-1 | N·s/m | 10,000 | 10,000 | 10,000 |
| | Axle-2–5 | N·s/m | 53,000 | 53,000 | 10,000 |
| Tire vertical stiffness | Axle-1 | N/m | 1500,000 | 1500,000 | 1750,000 |
| | Axle-2 | N/m | 3000,000 | 3000,000 | 3500,000 |
| | Axle-3 | N/m | 3000,000 | 3000,000 | 3500,000 |
| | Axle-4 | N/m | 3000,000 | 3000,000 | 3500,000 |
| | Axle-5 | N/m | 3000,000 | 3000,000 | 3500,000 |
| Tire damping coefficient | Axle-1–5 | N·s/m | 2,000 | 2,000 | 2,000 |
| Height of the gravity center $h$ | | m | 1.50 | 1.50 | 1.50 |
| $L_1$ | | m | 3.00 | 3.00 | 0.50 |
| $L_2$ | | m | 1.40 | 1.30 | 2.50 |
| $L_3$ | | m | 7.00 | 5.40 | 3.80 |
| $L_4$ | | m | 1.40 | 1.30 | 1.30 |
| $L_5$ | | m | 1.00 | 2.00 | 1.10 |
| $L_6$ | | m | 2.70 | 2.30 | 1.10 |
| $L_7$ | | m | 4.53 | 5.53 | 2.15 |
| $L_8$ | | m | 4.57 | 1.77 | 4.15 |
| $b$ | | m | 1.10 | 1.10 | 1.10 |

bridge were extracted and used in calculating the bridge responses based on the modal superposition approach. The fundamental frequency of the bridge was found to be 2.87 Hz.

Considering that heavy-duty trucks usually travel in slow lanes, the ATP in the simulation was loaded on the outside lane of the bridge, as illustrated in Fig. 5(a). In this case, the bottom of the Girder 3 at the mid-span is the most unfavorable position, from which the bending strains of the bridge were calculated for analysis.

### 3.3. Road surface profile model

Road surface condition is an important source of excitation for bridge vibration and can be modeled as a zero-mean stationary Gaussian random process. In this study, it was generated through an inverse Fourier transformation based on a dynamic spectral density (PSD) function as

$$r(x) = \sum_{k=1}^{N} \sqrt{2\varphi(n_k)\Delta n}\cos(2\pi n_k x + \theta_k) \tag{10}$$

where $r$ is the road profile; $\varphi()$ is the PSD function (m$^3$/cycle) for the road surface roughness; $n_k$ is the wavenumber (cycle/m); $\theta_k$ is a random phase angle uniformly distributed from 0 to 2π. In this study, the PSD function is referred to Ref. [40], and three classifications (i.e., Class-A, B, and C) of road roughness are considered according to the ISO specification [41].

### 3.4. Truck-road interface/tire model

Tires are the most important contact components between trucks and bridges, and the accuracy of tire models can significantly affect the interaction relationship between the truck and bridge [33]. A refined heavy-duty truck tire model [42] was developed in this section based on the physical characteristics of the typical truck tire, as shown in Fig. 6.

For each step of the iterative process of truck-bridge dynamic interaction, the tire deformations can be estimated as.

$$\Delta z_r(x,\ x_a) = \begin{cases} \left( r(x,x_a) + w(x,\ x_a) + \sqrt{R_0^2 - x_a^2} - R_0 - z(x) \right)\cdot\cos\theta & \Delta z \geqslant 0 \\ 0 & \Delta z < 0 \end{cases} \tag{11}$$

$$\cos\theta = \frac{R_0 - z(x)}{\sqrt{(x_a)^2 + (R_0 - z(x))^2}} \tag{12}$$

where $x$ is the position of the tire center line in the travel direction, $x_a$ is the relative contact position of the tire-road element to the centerline,$\theta$ is the angle between the center line and the radial tire element at $x_a$, and $\Delta z_r$ $(x,\ x_a)$ is the radial deformation of the corresponding contact element; $w$ is the deflection of the bridge; $R_0$ is the tire radius; $z$ is the overall deformation of the tire in the vertical direction. When $\Delta z_r < 0$, it indicates that the element is not in the contact patch and is therefore removed so that the length of the contact patch ($a$) can be determined. The deformation rates of the contact patch $\Delta \dot{z}_r$ can be calculated by

$$\Delta \dot{z}_r(x,\ x_a) = \left( \dot{r}(x,x_a) + \dot{w}(x,\ x_a) + \frac{x_a v}{\sqrt{R_0^2 - x_a^2}} - \dot{z}(x) \right)\cdot\cos\theta \tag{13}$$

in which $v$ is the vehicle speed. Thus, the vertical contact force of each tire acting on the bridge surface is

$$F(x) = n_b\cdot\sum^{n_a}\left( k_r(\cdot)\cdot\Delta z_r(x,x_a)\cdot\cos\theta\ + c_r(\cdot)\cdot\Delta\dot{z}_r(x,x_a)\cdot\cos\theta \right) \tag{14}$$

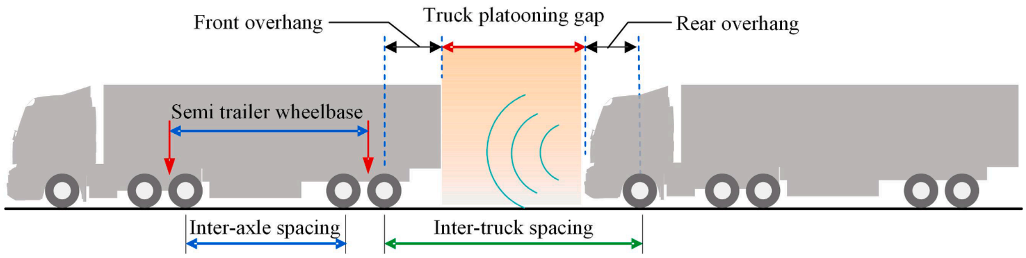


**Fig. 4.** The configuration of truck platooning.

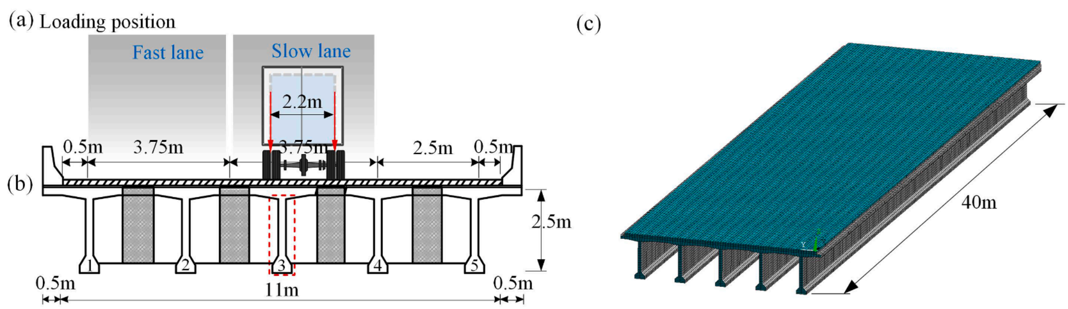


**Fig. 5.** Simply supported concrete T-girder bridge: (a) loading position of ATP on the bridge; (b) cross-section of the bridge; (c) finite element model of the bridge.

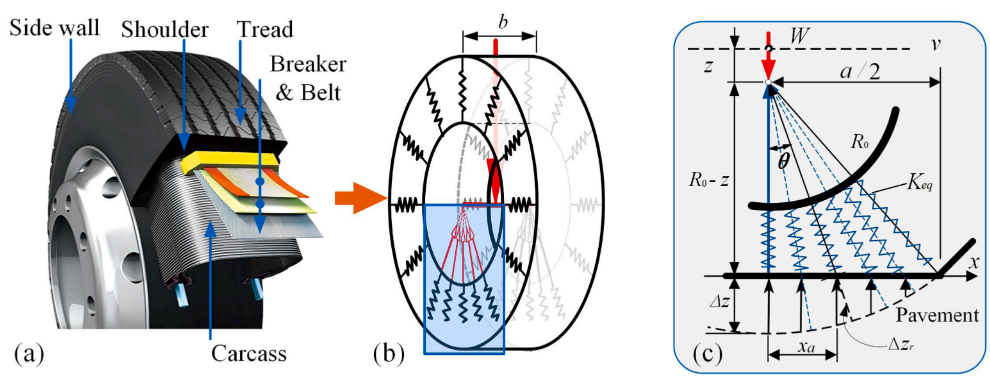


**Fig. 6.** Refined heavy-duty truck tire model: (a) structures of a typical truck tire; (b) diagram of the refined tire model; (c) calculation diagram in the contact patch.

in which

$$k_r(\cdot) = H_1(x_a)\cdot H_2\cdot K_t/(n_a\cdot n_b) \tag{15}$$

$$H_1(x, x_a) = 1 + \frac{\Delta z_r(x, x_a)}{\max\Delta z_r(x, x_a)} \tag{16}$$

$$c_r(\cdot) = C_t/(n_a\cdot n_b) \tag{17}$$

where $F$ is the vertical contact force of the tire; $k_r$ is the distributed radial stiffness coefficients of the contact elements along the contact patch; $H_1(x,\ x_a)$ is the modification function over the contact patch; $H_2$ is the conversion coefficient, taken as 1.5; $K_t$ is the vertical stiffness of the whole tire; $n_a$ is the number of contact elements in the travel direction, which is determined by Eq. (11); $n_b$ is the number of contact elements in the traverse direction. In this study, the length of each contact point in travel and transverse direction was taken as 0.01 m and 0.02 m, respectively; $c_r(\cdot)$ is the distributed radial damper coefficient, which is mainly determined by the hysteresis of tire materials. Thus $c_r(\cdot)$ can be simplified as a uniform distribution of the damper coefficient ($C_t$).

According to the actual situation, the steering axles of the truck were modeled as single-tire while the other axles were simulated based on a dual-tire assembly.

### 3.5. Truck-bridge interaction system assembly

The equations of motion for the vehicle and bridge are coupled through the tire contact forces. The equation of motion for the vehicle-bridge coupled system is

$$\begin{bmatrix} \boldsymbol{M}_b & \\ & \boldsymbol{M}_v \end{bmatrix}\begin{Bmatrix} \ddot{\boldsymbol{Y}} \\ \ddot{\boldsymbol{Z}} \end{Bmatrix}+\begin{bmatrix} \boldsymbol{C}_b+\boldsymbol{C}_{b-b} & \boldsymbol{C}_{b-v} \\ \boldsymbol{C}_{v-b} & \boldsymbol{C}_v \end{bmatrix}\begin{Bmatrix} \dot{\boldsymbol{Y}} \\ \dot{\boldsymbol{Z}} \end{Bmatrix}+\begin{bmatrix} \boldsymbol{K}_b+\boldsymbol{K}_{b-b} & \boldsymbol{K}_{b-v} \\ \boldsymbol{K}_{v-b} & \boldsymbol{K}_v \end{bmatrix}\begin{Bmatrix} \boldsymbol{Y} \\ \boldsymbol{Z} \end{Bmatrix}=\begin{Bmatrix} \boldsymbol{F} \\ \boldsymbol{F}\ +\boldsymbol{F}_v^G \end{Bmatrix} \tag{18}$$

where $\boldsymbol{M}$, $\boldsymbol{C}$, $\boldsymbol{K}$ are the matrices of mass, damping, and stiffness, respectively; the subscripts $b$ and $v$ represent the bridge and vehicle, respectively; $\boldsymbol{Y}$ and $\boldsymbol{Z}$ are the displacement of the bridge and vehicle, respectively; $\boldsymbol{C}_{b\text{-}b}$, $\boldsymbol{C}_{b\text{-}v}$, $\boldsymbol{C}_{v\text{-}b}$, $\boldsymbol{K}_{b\text{-}b}$, $\boldsymbol{K}_{b\text{-}v}$, $\boldsymbol{K}_{v\text{-}b}$ are the special terms due to the expansion of the tire contact forces vector $\boldsymbol{F}$, and the $\boldsymbol{F}_v^G$ is the tire contact force caused by gravity. After all the equations and matrices are developed and assembled according to Eq. (18), the Newmark-$\beta$ method is adopted to solve the overall truck platoon-bridge interaction system. The detailed solution process can be referred to Ref. [28].

## 4. Simulation and results

### 4.1. Simulation framework

Based on the refined VBI simulation system developed in the former section, numerical simulations were carried out within the framework displayed in Fig. 7. In the simulation, three kinds of road surface conditions (Class A–C) were considered, where the inter-truck spacings ranged from 2 to 15 m [13] at an interval of 1 m, and the truck speeds ranged from 0 to 120 km/h at an interval of 5 km/h. For each combination of inter-truck spacing, truck speed and road surface conditions, the dynamic responses of the bridge under the load of ATP composed of a different number of trucks were calculated for the three 5-axle trucks. To reduce the effect of the randomness of the artificial road profile samples, each simulation job was repeatedly simulated 20 times, and the average of the 20-times results was eventually taken as the effective result.

### 4.2. Dynamic impact description

Dynamic Load Allowance (DLA) [27] is usually used to characterize the additional load effect caused by the dynamic impact of vehicles. The DLA is defined as

$$\text{Dynamic load allowance} = \frac{R_{dyn} - R_{sta}}{R_{sta}} \tag{19}$$

in which, $R_{\text{sta}}$ and $R_{\text{dyn}}$ are the maximum static and dynamic response of the bridge, respectively, which refer to the maximum bending strain of the critical girder at the mid-span of the bridge.

Per the bridge design codes from China [26], the United States [27], and European Union [43], the code-specified DLAs for the bridge (40 m) analyzed in the present study are 0.17, 0.33, and 0.14, respectively.

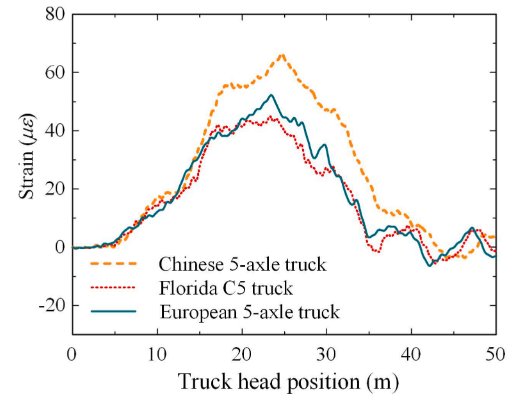


**Fig. 8.** Dynamic bending strains of the bridge under a single-truck scenario (moving at 80 km/h with Class-B road surface conditions).

### 4.3. Dynamic impact under single-truck scenario

The dynamic bending strain curves (strain/position) of the bridge under a typical single-truck scenario for the three 5-axle trucks are displayed in Fig. 8, of which the x-axis label “truck head position” refers to the relative position of the front axle of the truck to the bridge entrance. As illustrated in Fig. 8, the bending strains induced by the Chinese 5-axle truck are the largest in terms of amplitude, and then followed by the European 5-axle truck and the Florida C-5 truck. This difference depends on the variance of gross weight and axle-load distribution of the three trucks. Overall, the dynamic components of the dynamic bending strains of the bridge under the single-truck scenario are not significant, even for a truck speed of 80 km/h and Class-B road surface conditions.

To quantify the dynamic impact on the bridge under single-truck scenarios, Fig. 9 shows the calculated DLAs of the bridge under different combinations of truck speed and road surface conditions for the three trucks. The DLAs caused by the Chinese 5-axle truck and the Florida C5 truck demonstrate a clear increasing trend with the increase of truck speed, whereas the trend for the European 5-axle truck is not clear. It can be explained by the effect of speed on the vehicle-bridge

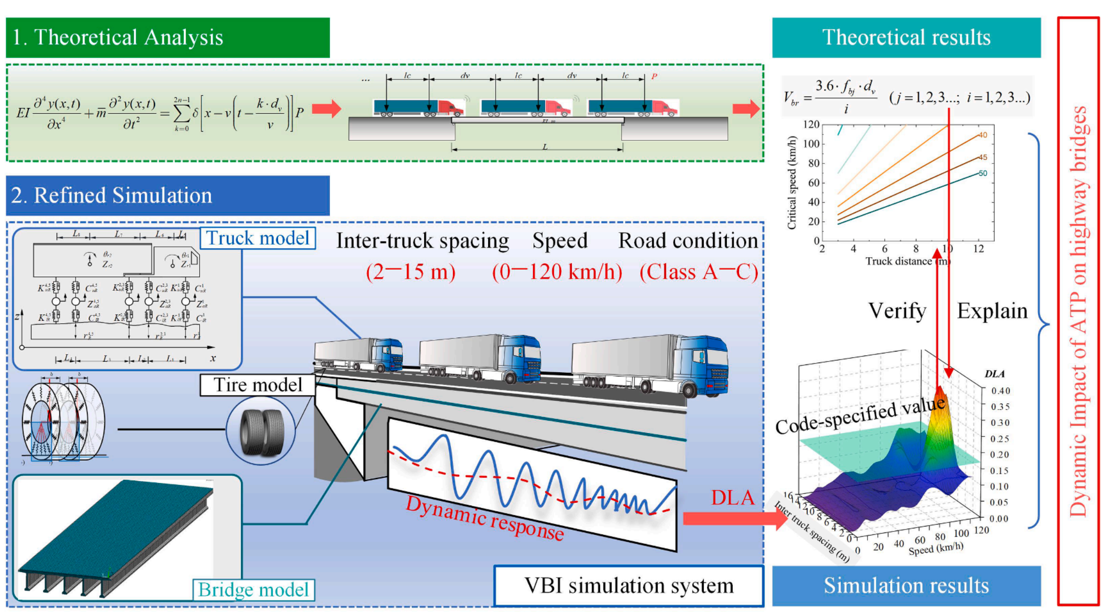


**Fig. 7.** Numerical simulation framework.

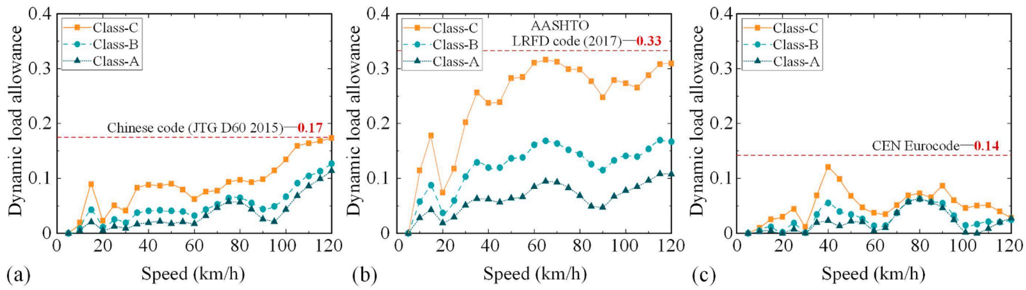


**Fig. 9.** Dynamic load allowances of the bridge under the single-truck load of (a) Chinese 5-axle truck, (b) Florida C5 truck, and (c) European 5-axle truck.

coupling vibration [19]. By comparison, the DLAs caused by the Florida C5 truck are significantly greater than those caused by the other two trucks. It is because the gross weight of the Florida C5 truck is relatively smaller, as introduced previously, and usually a lighter vehicle produces larger DLAs than a heavier one [19]. Based on the simulation results, all the DLAs induced by the three trucks have not exceeded the respective code-recommended values, even when the bridge surface is in a worse condition (Class-C).

### *4.4. Dynamic impact under truck platooning scenario*

The maximum dynamic response of the bridge can effectively reflect the dynamic impact of the truck platooning load. Accordingly, Fig. 10 shows the maximum bending strains of the bridge under truck platooning scenarios (with different combinations of inter-truck spacing and truck speed) for the three 5-axle trucks. To obtain the general rules, Fig. 10 only presents the results under four-truck platooning scenarios with Class-B road surface conditions. As previously mentioned, the sampling intervals of the truck speed and inter-truck spacing are 5 km/h and 1 m, respectively. The maximum bending strains for the combinations not sampled were obtained using linear interpolation. Overall, the maximum bending strains of the bridge under truck platooning scenarios increased slightly with the increase of vehicle speed but decreased significantly with the increase of the inter-truck spacing. This overall trend is quite reasonable and proves the efficiency of spacing control in reducing the load effect on highway bridges. However, it is noteworthy that the maximum bending strains of the bridge peak at critical truck speeds (identified by dashed red line/face), destroying the overall trend previously summarized. Taking Fig. 10(a) for an example, when the four-truck platoon is moving at 85 km/h, the induced maximum bending strains of the bridge for some inter-truck spacings (>9 m) are significantly increased and even close to that for the inter-truck spacing of 6 m. Similar phenomena can be observed in the other subfigures of Fig. 10. It is because the additional dynamic load effects caused by ATP under those critical loading scenarios outweigh the reduced load effects by merely enlarging inter-truck spacing, indicating that the method [16] of increasing the inter-truck spacing of ATP to reduce the additional load effect on highway bridges may not be reliable.

#### *4.4.1. Resonance condition identification and validation*

According to Section 2, the dynamic response of the bridge will be amplified when the ATP load pattern satisfies resonance conditions. To validate this speculation and figure out the peak-related phenomena in Fig. 10(a)–(c), the maximum bending strains of the bridge under different inter-truck spacings are plotted for each critical truck speed (identified from the upper part of Fig. 10(a)–(c)), and the maximum bending strains at 5 km/h are also plotted as static references, as shown in Figs. 11–13, in which the results of the ATP composed of 1–4 trucks are considered.

The maximum bending strains at 5 km/h (Figs. 11–13, connected by a solid interpolating line) are nearly linearly reduced as the inter-truck spacing increases, until the inter-truck spacing is larger than 9 m. For the same combinations of inter-truck spacing and truck speed, the maximum bending strain of the bridge caused by ATP will not be further amplified when the ATP is composed of more than two trucks. It indicates that ATP has a limited impact on the bridge in terms of the static load effect, and the additional static load effect could be removed by

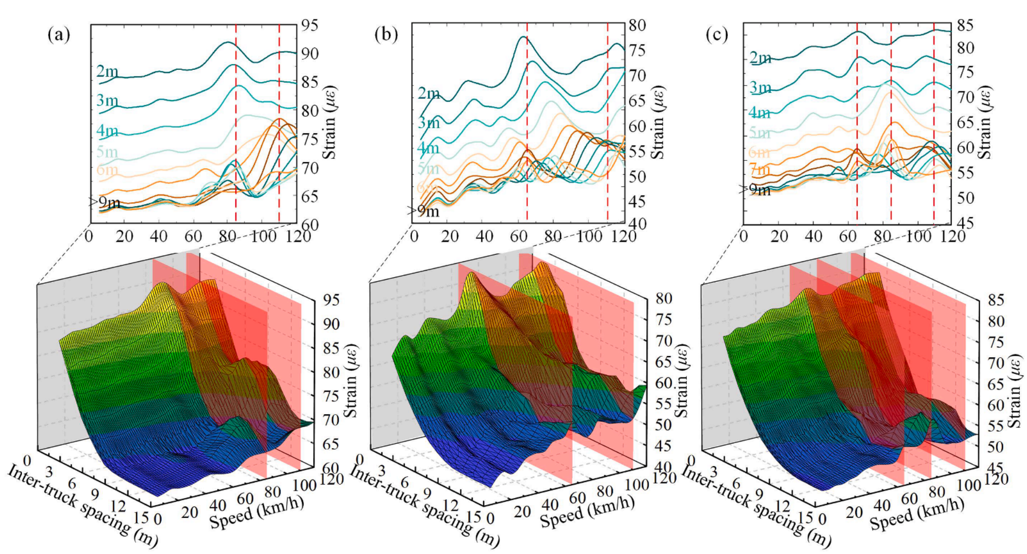


**Fig. 10.** The maximum bending strains of the bridge under the load of the four-truck platoon for a different combinations of truck speed and inter-truck spacing: (a) Chinese 5-axle truck; (b) Florida C5 truck; (c) European 5-axle truck.

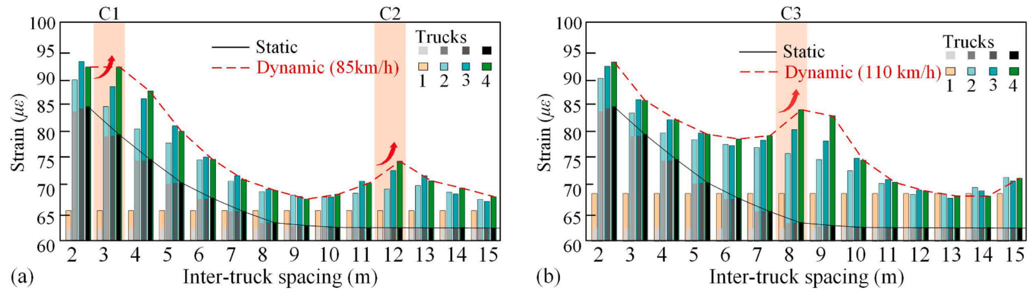


**Fig. 11.** The maximum bending strain of the bridge under the load of the Chinese 5-axle truck. (a) 85 km/h; (b) 110 km/h.

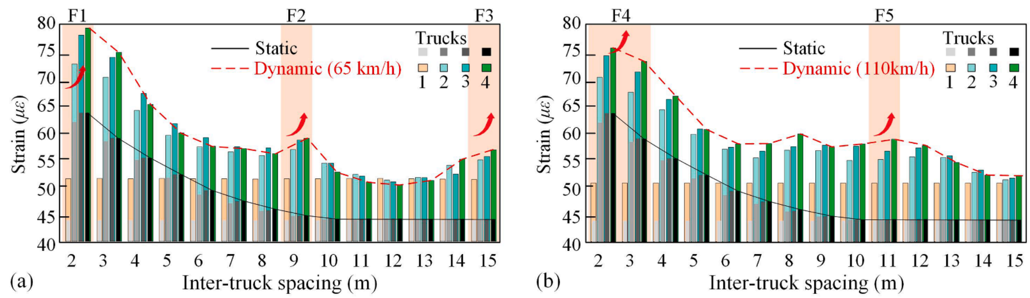


**Fig. 12.** The maximum bending strain of the bridge under the load of the Florida C5 truck. (a) 65 km/h; (b) 110 km/h.

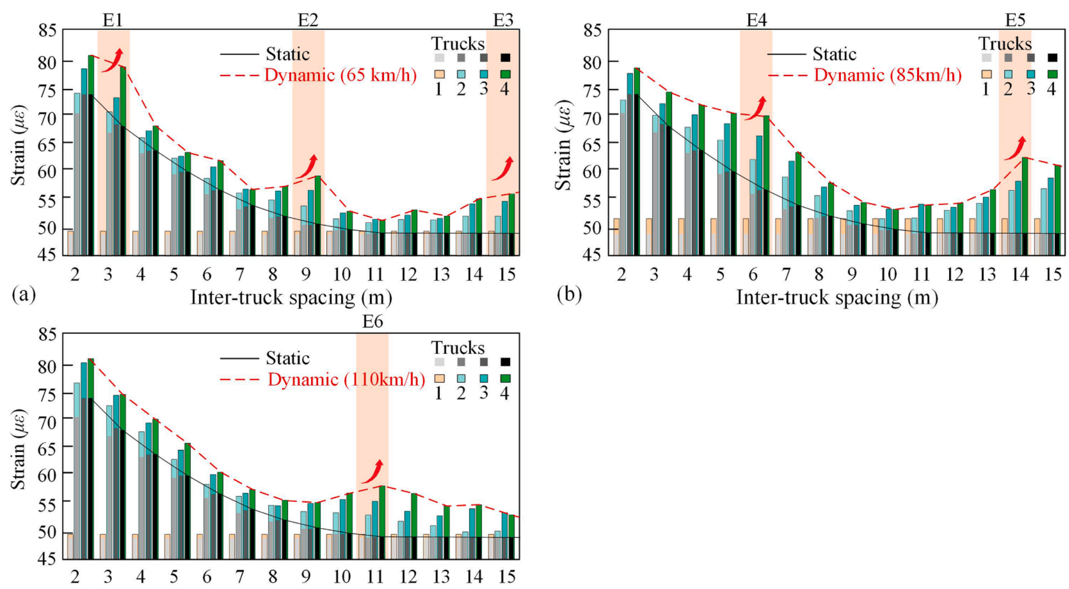


**Fig. 13.** The maximum bending strain of the bridge under the load of the European 5-axle truck. (a) 65 km/h; (b) 85 km/h; (c) 110 km/h.

increasing the inter-truck spacing to a certain value, which depends on the specific span length of the bridge.

As to the maximum bending strains at critical speeds (Figs. 11–13, red dotted line), they are undermined by notable peaks at specific inter-truck spacings. For those inter-truck spacings, the magnitudes of the maximum bending strain of the bridge are amplified by the number of trucks in the ATP, as marked using red arrows, resulting in significantly larger maximum bending strains than those in static scenarios. Accordingly, all those peak-related combinations of inter-truck spacing and truck speed from Fig. 10(a)–(c) can be identified, as listed in Table 3.

Substituting all the identified truck speeds and inter-truck spacings, along with the fundamental frequency of the bridge (2.87 Hz) and truck axle information into Eq. (9), the multipliers are estimated as shown in Table 3, which indicated the specific resonance conditions. The results showed that all those calculated multipliers for the identified combinations of truck speed and inter-truck spacing are near integers, implying that fractional harmonic resonance conditions are satisfied. Thus, all those peak-related phenomena in Fig. 11 are confirmed to be induced by bridge resonance, which can be reasonably predicted by the theoretical equation of Section 2.

#### *4.4.2. Typical bridge responses in resonance condition*

For illustration, Fig. 14(a)–(c) showed the typical bending strain curves of the bridge under the typical resonance conditions of C1, C2, and C3, respectively. It reflects the increasing trend of the bending strain

**Table 3**
Validation of resonance condition.

| Truck (Overall length) | Loading Case | Combination | | The multiplier for all axle loads | | The multiplier for effective wheel loads | |
|---|---|---|---|---|---|---|---|
| | | Speed (km/h) | Spacing (m) | Calculated | Theoretical | Calculated | Theoretical |
| Chinese 5-axle truck | C1 | 85 | 4 | 2.04 | 2 | 1.02 | 1 |
| (12.8 m) | C2 | 85 | 12 | 3.01 | 3 | 1.02 | 1 |
| | C3 | 115 | 8 | 1.87 | 2 | 0.75 | — |
| Florida C5 truck | F1 | 65 | 2 | 2.07 | 2 | 1.05 | 1 |
| (11 m) | F2 | 65 | 9 | 3.18 | 3 | 1.05 | 1 |
| | F3 | 65 | 15 | 4.13 | 4 | 1.05 | 1 |
| | F4 | 110 | 2/3 | 1.22 | 1 | 0.62 | — |
| | F5 | 110 | 11 | 2.07 | 2 | 0.62 | — |
| European 5-axle truck | E1 | 65 | 3 | 2.11 | 2 | 0.94 | 1 |
| (10.3 m) | E2 | 65 | 9 | 3.07 | 3 | 0.94 | 1 |
| | E3 | 65 | 15 | 4.02 | 4 | 0.94 | 1 |
| | E4 | 85 | 6 | 1.98 | 2 | 0.72 | — |
| | E5 | 85 | 14 | 2.95 | 3 | 0.72 | — |
| | E6 | 115 | 11 | 1.91 | 2 | 0.53 | — |

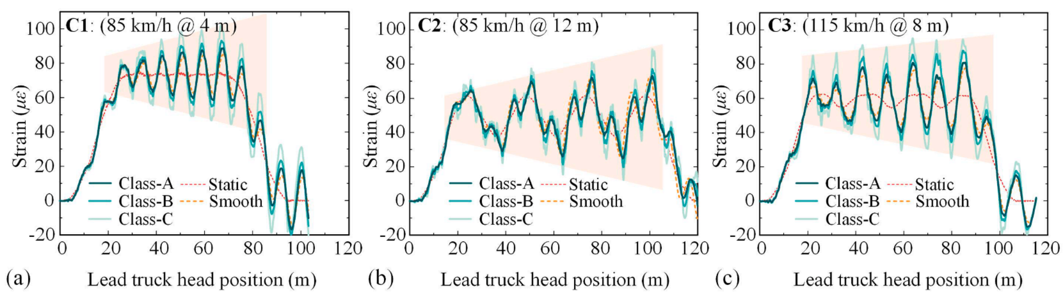


**Fig. 14.** Typical bending strain curves of the bridge under the load of the four-truck platoon composed of the Chinese 5-axle truck, (a) moving at 85 km/h with an inter-truck spacing of 3 m; (b) moving at 85 km/h with inter-truck spacing of 12 m; (c) moving at 110 km/h with an inter-truck spacing of 8 m.

of the bridge under the periodic load of ATP. The superposition effect is significant even when the road surface condition is smooth. That is because the superposition states of the dynamic responses of the bridge are completely determined by the ATP-specified loading frequency, as the fundamental frequency of the bridge is fixed. Additionally, the worse the road surface condition is, the more significant the superposition effects are. Because the basic amplitude of the bridge response caused by each truck can be greatly affected by the road roughness [19]. Based on the above analysis, the maximum dynamic responses of the bridge in ATP-induced resonance conditions appear to be amplified by both the road surface conditions and the number of trucks, they would therefore be significantly larger than those under non-resonance loading scenarios, including the single-truck loading scenarios demonstrated in Fig. 8. Since the maximum dynamic responses are directly related to the calculation and evaluation of the DLA of the bridge, it is reasonable to challenge the current code-specified DLAs, which mainly account for one truck-induced impact on the bridge at a time, which may not be sufficient to characterize the impact from the ATP load, particularly in resonance conditions.

### 4.5. DLAs of the bridge in resonance conditions

Related to Fig. 10, the DLAs of the bridge under the same truck platooning scenarios are calculated for the three trucks, as illustrated in Fig. 15, in which the road surface conditions of Class-B is considered to represent a normal road condition. It is notable to see that the DLAs of the bridge in some resonance conditions exceed the current code-specified values, especially for the Chinese code (Fig. 15(a)) and Eurocode (Fig. 15(c)), from which the DLAs are suggested with relatively small values but found to be exceeded to a large extent. The extent may be expanded for the bridges with a lower fundamental frequency, because those bridges are generally recognized to have smaller DLAs but are prone to ATP-induced resonances. The DLA suggested in the *AASHTO LRFD specification* (2017) is recognized to be generally more

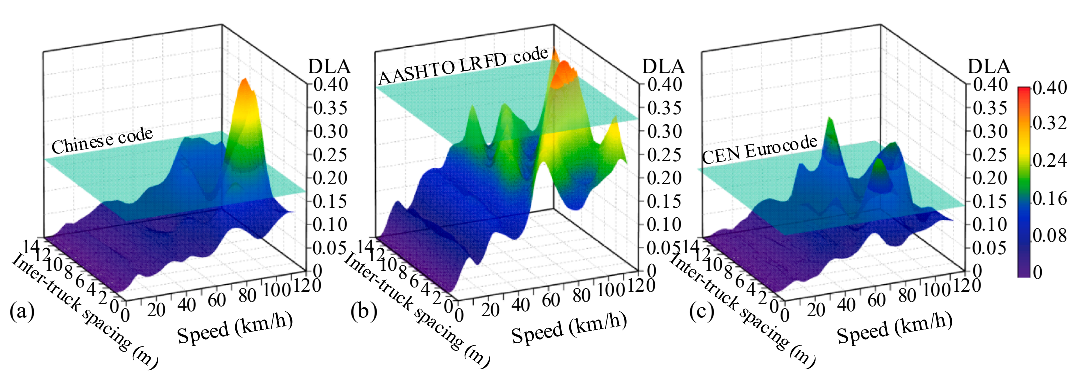


**Fig. 15.** DLAs of the bridge under the load of four-truck platoon: (a) Chinese 5-axle truck; (b) Florida C5 truck; (c) European 5-axle truck.

conservative, but it can still be exceeded under some resonance conditions (Fig. 15(b)). It contrasts with the finding of Fig. 8, in which all the DLAs obtained under single-truck scenarios are within the code-specified values even when the road surface is in Class-C condition. Therefore, for highway bridges, the ATP-induced resonance scenarios can be regarded as a new critical loading case, under which a larger DLA may be induced. Besides, with a poor road surface condition or a large number of trucks in the ATP, the DLAs of the bridge can be further amplified, exceeding the current code-specified DLAs.

It should be emphasized that in the preliminary study conducted, the fundamental frequency of the bridge was identified as the key factor in predicting bridge resonances, and the resonance conditions in simulation can be reasonably predicted. Since the focus of this study is to provide recommendations for the management of ATP, the simulation results were then discussed focused on the effect of truck platooning behaviors with different combinations of truck speed and inter-truck spacing.

#### 4.5.1. *Effect of number of trucks*

Figs. 16–18 show the predicted DLAs of the bridge under the load of ATP composed of a different number of trucks at different road roughness for the typical resonance conditions previously identified. As shown in Figs. 16–18, the DLAs of the bridge under the typical resonance conditions increase significantly with the number of trucks. Overall, the worse the road surface condition is, the more significant the increasing trends are. The increasing trends seem to slow down after the ATP is extended to a certain scale, which may be explained by the bridge damping effect and the change of boundary conditions [38]. As a result, all the current code-specified DLAs of the bridge can be exceeded to a large extent. They highlight the necessity of limiting the size of the ATP and modifying the code-specified DLAs. Because modifying the code-specified DLA of the bridge to accommodate the emerging ATP with the unlimited size is of no practical use and may be unrealistic. On the contrary, only limiting the size of ATP may not be effective since the current code-suggested DLA can be exceeded even when a two-truck platoon crosses the bridge regardless of the road surface conditions, such as the loading cases C3 and E5. They indicate that ATP-induced bridge resonances play a dominant role in determining the DLAs of existing highway bridges. To reduce the potential adverse impact, both measures of modifying the code-specified DLA and limiting the scale of ATP should be considered.

#### 4.5.2. *Effect of inter-truck spacing*

Promoted by the low-latency V2V technology, the inter-truck spacing of a truck platoon can be flexibly controlled. Thus, a series of bridge resonance conditions will be satisfied by one resonance speed combined with different inter-truck spacings (e.g., F1, F2, F3). In that case, the DLA for the condition of larger inter-truck spacing (representing low-order fractional harmonic resonance) is found not necessarily lower than the DLA of a smaller spacing condition (near ideal resonance). It is mainly because the closer inter-truck spacings usually correspond to the larger static load effects, which would in turn result in lower calculated DLAs. Besides, it usually requires a significant spacing adjustment for the ATP load changing from one resonance condition to an adjacent resonance condition. For example, when the inter-truck spacing of the ATP increases from 4 m to 12 m, the resonance condition is only transited from C1 to C2, representing the bridge response overlay at 1-cycle interval to 2-cycle interval. However, the amplitude attenuation of bridge vibration for a short cycle time is weak due to the low structural damping. In summary, increasing the inter-truck spacing can significantly reduce the static load effect but may have little influence on the dynamic load effect on a bridge, thus resulting in a larger DLA. This conclusion further emphasizes that the traditional method of increasing truck headway to reduce the load effect is not fully applicable to ATP scenarios, especially in ATP-induced resonance conditions. It also implies that, as long as limiting the inter-truck spacings of the ATP, the requirement of adjusting design loading (lane-loading) in the bridge design code can be avoided. Nonetheless, the current code-specified DLA may still be questionable, and more assessments should be carried out for various highway bridges under the ATP loads, particularly in resonance conditions.

## 5. Bridge resonance control

As discussed previously, those passive methods such as maintaining the road surface conditions, increasing the inter-truck spacing, and limiting the number of trucks cannot eliminate those adverse dynamic impacts. Modifying the code-specified DLA might be effective but may result in a massive amount of follow-up work.

### 5.1. *Cancellation of the bridge resonance*

According to Eq. (9), bridge resonance occurs when the time interval between two adjacent axle loads of the ATP is *i* (integer) times of the natural period of the bridge. It is easy to infer that if the ratio of the loading period of the ATP to the natural period of the bridge is not an integer, the load effect from each axle can be counteracted and even be canceled entirely. Thus, the cancellation conditions can be deduced as.

$$V_{bc} = \frac{7.2 \cdot f_{bj} \cdot dv}{2i-1} \qquad (j = 1, 2, 3 \ldots; i = 1, 2, 3 \ldots; j \neq 2i-1) \tag{20}$$

Based on the fundamental frequency of the bridge (2.87 Hz) and the known overall wheel spacing of the three kinds of trucks (12.8 m, 11.0 m, 10.3 m), the resonance and cancellation conditions for some multipliers, *i*, are identified by Eq. (9) and Eq. (20), respectively, as shown in Fig. 19.

It can be seen from Fig. 19 that the line markings of the resonance/cancellation conditions for different multipliers are scattered among various speeds. The line-markings regarding lower multipliers (i.e., $i$ = 2, 3) are distributed sparsely and more inclined to occur at relatively high speed, and vice versa. As the multiplier increases ($i > 3$), the line-marking of the resonance and cancellation conditions approach each other. Thus, a slight adjustment of the truck speed in the low-speed range may lead to the alternating fulfillment of multiple resonances and cancellation conditions. Nevertheless, the resonance conditions for the lower multiplier should be paid much attention to, because the resonance vibrations of the bridge under those conditions are

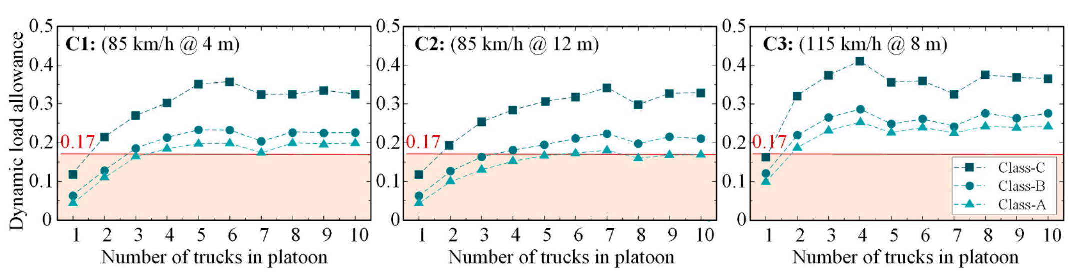


**Fig. 16.** DLAs of the bridge versus an increased number of trucks in the platoon for typical resonance conditions (Chinese 5-axle truck).

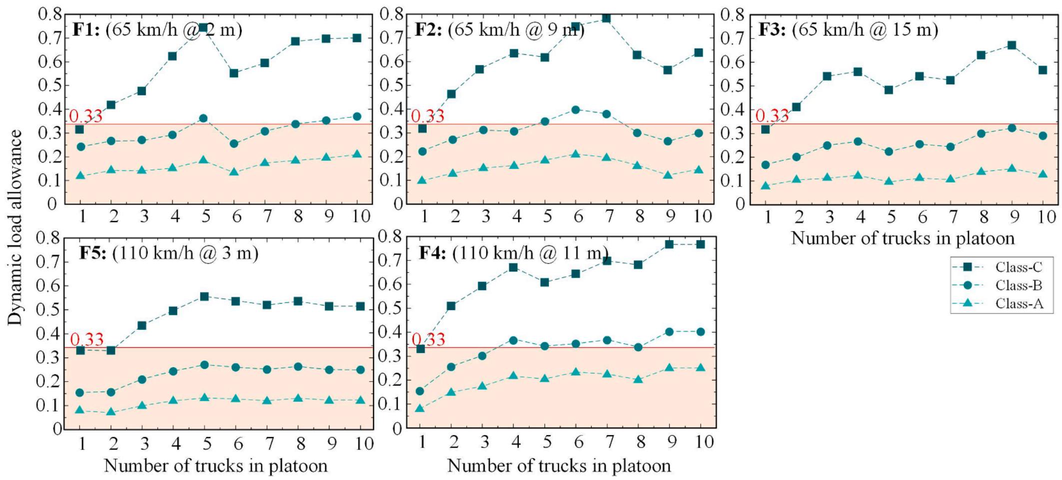


**Fig. 17.** DLAs of the bridge versus an increased number of trucks in the platoon for typical resonance conditions (Florida C5 truck).

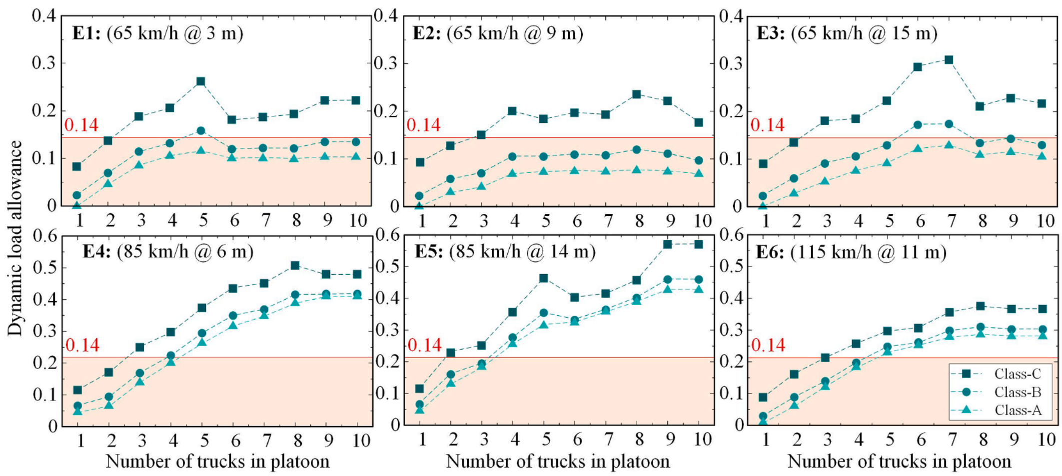


**Fig. 18.** DLAs of the bridge versus an increased number of trucks in the platoon for typical resonance conditions (European 5-axle truck).

significant, and those conditions are also prone to occur at high speeds, which further amplify the bridge vibrations.

For comparison, the contour plot of the simulated DLAs of the bridge under the load of four-truck platoons moving with Class-B road roughness is also displayed in Fig. 19. It can be seen that:

(1) Overall, the resonance conditions identified from the simulated DLAs are consistent with the theoretical results. All the relatively larger DLAs are distributed around the resonance conditions (Fig. 19, solid red line-marking), while the DLAs near the cancellation combinations (Fig. 19, long dash line-marking) are truly small;
(2) The resonance effects quantified by DLAs vary with the resonance conditions (special combinations of the inter-truck spacing and truck speed), even for those combinations that belong to the resonance conditions with the same multiplier;
(3) Not all the calculated DLAs distributed over the resonance line-markings are significant. Only when the truck speed exceeds a limit, the DLAs of the bridge around the resonance line-markings are significantly increased, and greater DLAs are usually prone to occur at higher speeds. The probable reason will be described in the following Section 5.2.

### 5.2. Speed threshold

As shown in Fig. 19, the speed limit can be recognized as a speed threshold (marked by short-line dashes) for the ATP to induce critical resonance. The speed threshold divides the operation speed range into a safe zone and a resonance zone.

It is found that the speed threshold for each truck is almost completely equal to the corresponding minimum critical resonance speed identified in Fig. 10. It is because the bridge responses at those resonance speeds are accumulated not only by the axles from different trucks, but also by the front and rear axles (groups) from the same truck. For example, when the ATP (Chinese 5-axle truck) is moving at 85 km/h with the inter-truck spacing of 4 m, it satisfies the condition of 1/2 fractional harmonic resonance in terms of the front or rear axle loads from different trucks, as shown in Table 2. Meanwhile, Considering the effective wheel loads from the same truck and neglecting the steering axle load, the result of adding the inter-truck spacing (4 m) to the trailer wheelbase (3 m) is quite close to the effective wheelbase of the tractor (8.4 m), as demonstrated in Fig. 20(a). In this case, the superposition effect of the front and rear axle loads from one truck is maximized. It essentially fulfills the co-frequency resonance condition for the bridge, resulting in a significant bridge vibration even at a relatively low resonance speed. A similar finding can be obtained when the inter-truck spacing is 12.8 m, as shown in Fig. 20(b).

Therefore, the identified minimum critical resonance speed can be

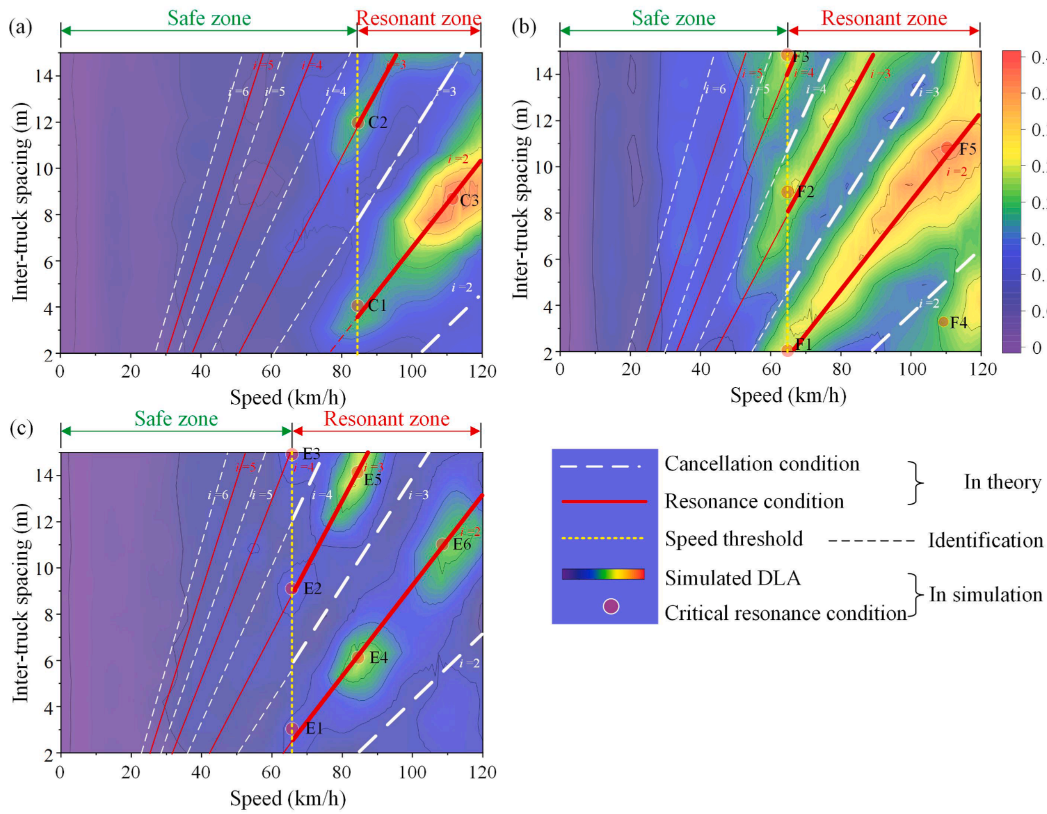


**Fig. 19.** Resonance and cancellation conditions of the bridge: (a) Chinese 5-axle truck; (b) Florida C5 truck; (c) European 5-axle truck.

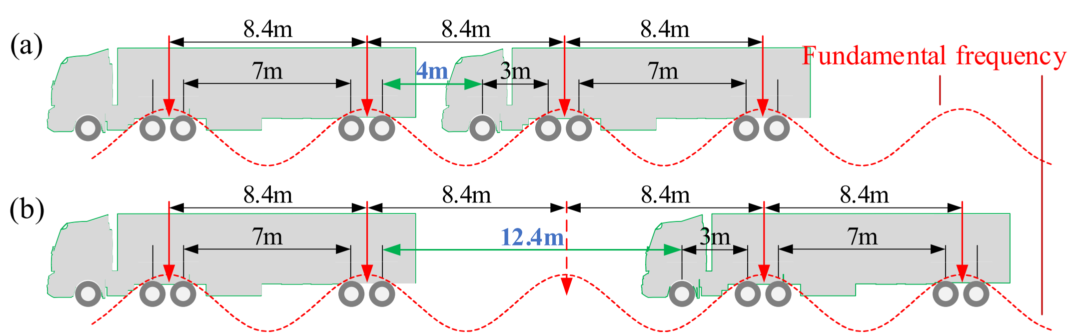


**Fig. 20.** Description of the resonance condition associated with the speed threshold (Chinese 5-axle truck displayed). (a) Moving at 85 km/h, spacing of 4 m; (b) moving at 85 km/h, spacing of 12.4 m.

reasonably recognized as the speed threshold to induce a notable bridge resonance response. On the contrary, when the resonance speeds are within the speed threshold, the resonance effect is not obvious since the dynamic load effect caused by each axle load at this speed is relatively small. Besides, the resonance conditions regarding low speeds are quite closer to the cancellation conditions, which play a dominant role in determining bridge vibration. As for the situations of resonance speed exceeding the speed threshold, the dynamic response of the bridge induced by every single axle is significant. Moreover, the increased loading frequency makes the superposition effect between two adjacent axles (groups) more significant. All these factors contribute to the more significant resonance effects for higher resonance speeds.

Accordingly, the speed threshold can be reasonably identified by substituting the fundamental frequency of the bridge and the effective wheelbase (spacing between the heavy axles/groups) of the truck into Eq. (9). This rule also applies to other freight trucks.

### 5.3. Optimal strategy for ATP crossing highway bridges

For practical purposes, based on the previous discussion, an optimal traffic strategy is proposed for the ATP to manage the operation models before crossing the highway bridges, as illustrated in Fig. 21.

(1) Bridge fundamental frequency is unknown
- Step 1: Maintain the road surface conditions and avoid other adverse factors that motivate the truck vibration;
- Step 2: Limit the number of trucks of the ATP to no greater than 3;
- Step 3: Ensure the inter-truck spacing of the ATP greater than 9 m to avoid the additional static load effect on the bridge;
- Step 4: Reduce the truck speed as small as legally possible (generally not below the legal low-speed limit of 60 km/h).

(2) Bridge fundamental frequency has been measured
- Step 1: Ensure the inter-truck spacing of the ATP larger than 9 m to avoid the additional static load effect of the bridge;

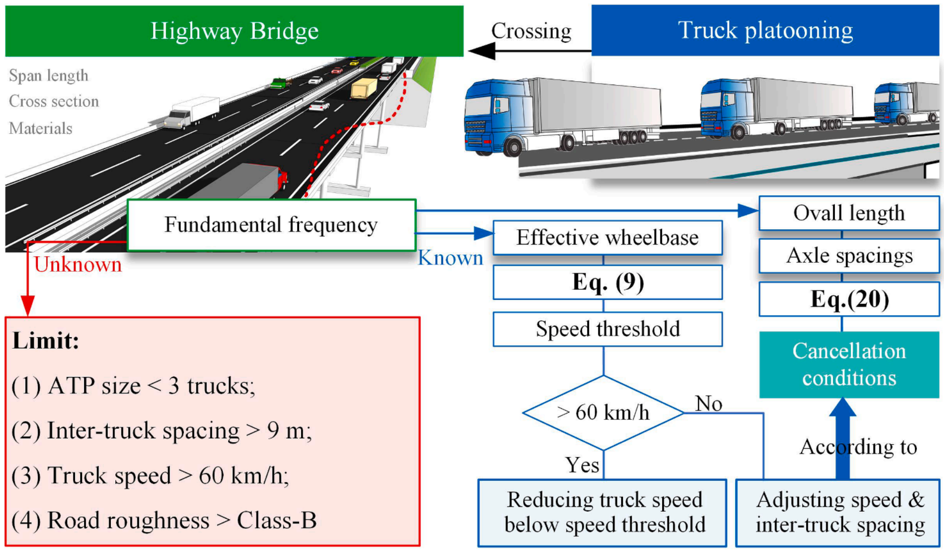


**Fig. 21.** The optimal strategy for ATP crossing highway bridges.

- Step 2: Identify the effective wheelbase of the truck, then combine it with the known bridge fundamental frequency to determine the speed threshold via Eq. (9);
  - o If the speed threshold exceeds the legal low-speed limit (60 km/h), maintain the truck speed between the legal low-speed limit and the speed threshold;
  - o If the identified speed threshold is lower than the legal low-speed limit (60 km/h), compare the current loading frequency of the ATP with the fundamental frequency of the bridge.
- Step 3: Manage the current combination of truck speed and inter-truck spacing according to the cancellation conditions identified by Eq. (20).

In general, automatically modifying the operating states of the ATP according to cancellation conditions is the most effective method to reduce the accompanying adverse dynamic impact on highway bridges. To this end, adjusting the speed simultaneously for all trucks is of more practical value, since changing the inter-truck spacing is a time-consuming process that also relies on the change of speed. Nevertheless, it always prefers to maintain the ATP at a relatively low speed, as long as the speed is within the legal speed limit.

## 6. Summary and conclusions

In this study, the potential dynamic impact on highway bridges from the emerging automated truck platooning (ATP) has been theoretically analyzed and numerically investigated. The following conclusions can be drawn:

(1) The emerging ATP consisting of common heavy-duty trucks can produce adverse dynamic load effects on existing highway bridges, particularly for the medium-to-long span bridges that have a fundamental frequency below 6.5 Hz. Since these bridges are prone to resonate with severe vibration when the ATP crosses, further investigation is needed to quantify the adverse impact for design purposes.

(2) The DLAs suggested in current bridge design codes may not be sufficiently capable of characterizing the dynamic effects brought by ATP. When the inter-truck spacing of the ATP satisfied a certain relationship with the truck speeds, bridge resonance would occur and may thus result in larger DLAs against current code-specified values. The DLAs would also be amplified by the number of trucks and be greatly affected by the road roughness. To prevent such adverse situations, limiting the truck platoon size is found to be an important approach based on numerical simulations.

(3) The traditional method of reducing the load effect of ATP by merely increasing the inter-truck spacing is not entirely reliable. It is found that a series of bridge resonance conditions could be induced when combining the normal truck speed with multiple inter-truck spacings. Those resonance conditions associated with larger inter-truck spacing may result in a more significant dynamic impact on bridges. Therefore, toward decreasing the additional overall load effect from the ATP, avoiding resonance should also be an important principle.

(4) Managing the automated truck platooning across the highway bridges according to cancellation conditions is the most effective method of eliminating bridge resonance and reducing the related adverse impact. To this end, the fundamental frequency of the bridge should better be tested or roughly estimated in advance, so that all the cancellation conditions can be predicted by the cancellation formula, and the speed threshold could also be identified by substituting the bridge fundamental frequency and the truck axle configuration into the resonance formula. Therefore, the speed of the ATP can be managed according to the cancellation conditions or at least be maintained below the specified speed threshold, to reduce the dynamic impact on the highway bridges.

The present study focused on exploring and revealing the potential dynamic impact induced by ATP on highway bridges, which is important to the highway bridge/truck platoon stakeholders. The theoretical findings and developed analysis framework in this study can serve as a basis for further investigations on the bridge structural requirements and traffic limitations associated with the ATP. Based on this study, various types of bridges in the highway network could be evaluated regarding the critical resonance conditions through simulation or experimental studies.

### *CRediT authorship contribution statement*

**Tianyang Ling:** Methodology, Software, Data curation, Visualization, Investigation, Writing – original draft. **Ran Cao:** Validation, Investigation, Supervision, Writing – review & editing. **Lu Deng:** Conceptualization, Methodology, Supervision, Writing – review &

editing, Project administration, Funding acquisition. **Wei He:** Software, Supervision, Visualization, Writing – review & editing. **Xin Wu:** Investigation, Project administration. **Wenjie Zhong:** Investigation, Writing – review & editing.

## Declaration of competing interest

The authors declare that they have no known competing financial interests or personal relationships that could have appeared to influence the work reported in this paper.

## Acknowledgments

This research was funded by the National Natural Science Foundation of China (51778222, 52008160, 52108139), the Key Research and Development Program of Hunan Province of China (2017SK2224), and the Hunan Provincial Science & Technology Leading Innovator Program (2021RC4025).

## References

[1] Tsugawa S, Jeschke S, Shladover SE. A review of truck platooning projects for energy savings. IEEE Trans Intell Veh 2016;1(1):68–77. https://doi.org/10.1109/TIV.2016.2577499.

[2] Jacob B, De Chalendar OA. Truck platooning: expected benefits and implementation conditions on highways. In: Pauwelussen JP, Aarts L, editors. Book of Technical Papers of the 15th International Symposium on Heavy Vehicle Transport Technology (HVTT 15); 2018 Oct 2–5; Rotterdam, Netherlands. Arnhem: HAN Automotive; 2019. p. 1–11.

[3] Birgisson B, Morgan C, Yarnold M, Warner J, Glover B, Steadman M, et al. Evaluate potential impacts, benefits, impediments, and solutions of automated trucks and truck platooning on Texas highway infrastructure: technical report. Report. Washington: U.S. Department of Transportation Federal Highway Administration; 2020 Aug. Report No.:FHWA/TX-21/0-6984-R1, 0-6984-R1.

[4] Alam A, Besselink B, Turri V, Martensson J, Johansson KH. Heavy-duty vehicle platooning for sustainable freight transportation: a cooperative method to enhance safety and efficiency. IEEE Control Syst 2015;35:34–56. https://doi.org/10.1109/MCS.2015.2471046.

[5] Saeed TU, Alabi BNT, Labi S. Preparing road infrastructure to accommodate connected and automated vehicles: system-level perspective. J Infrastruct Syst 2021;27:06020003. https://doi.org/10.1061/(ASCE)IS.1943-555X.0000593.

[6] Calvert SC, Schakel WJ, van Arem B. Evaluation and modelling of the traffic flow effects of truck platooning. Transp Res Part C Emerg Technol 2019;105:1–22. https://doi.org/10.1016/j.trc.2019.05.019.

[7] Othman K. Impact of autonomous vehicles on the physical infrastructure: changes and challenges. Designs 2021;5:40. https://doi.org/10.3390/designs5030040.

[8] Sayed SM, Sunna HN, Moore PR. Truck platooning impact on bridge preservation. J Perform Constr Facil 2020;34:04020029. https://doi.org/10.1061/(asce)cf.1943-5509.0001423.

[9] Chen F., Song M., Ma X. A lateral control scheme of autonomous vehicles considering pavement sustainability. J Clean Prod 2020; 256: 120669. https://doi.org/10.1016/j.jclepro.2020.120669.

[10] Gungor OE, Al-Qadi IL. All for one: centralized optimization of truck platoons to improve roadway infrastructure sustainability. Transp Res Part C Emerg Technol 2020;114:84–98. https://doi.org/10.1016/j.trc.2020.02.002.

[11] Chen F, Song M, Ma X, Zhu X. Assess the impacts of different autonomous trucks' lateral control modes on asphalt pavement performance. Transp Res Part C Emerg Technol 2019;103:17–29. https://doi.org/10.1016/j.trc.2019.04.001.

[12] Song M, Chen F, Ma X. Organization of autonomous truck platoon considering energy saving and pavement fatigue. Transp Res Part D Transp Environ 2021;90:102667. https://doi.org/10.1016/j.trd.2020.102667.

[13] DeVault A, Beitelman TE. Two-truck platooning: load effects of two-truck platoons on interstate and turnpike bridges in Florida. Rep to Florida Dept Transp (FDOT). Oviedo: FDOT Office Maintenance; 2016.

[14] Kamranian Z. Load evaluation of the Hay River Bridge under different platoons of connected trucks. [dissertation]. Calgary: University of Calgary; 2018.

[15] Couto Braguim T, Lou P, Nassif H. Truck platooning to minimize load-induced fatigue in steel girder bridges. Transp Res Rec J Transp Res Board 2021;2675(4):146–54.

[16] Yarnold MT, Weidner JS. Truck platoon impacts on steel girder bridges. J Bridg Eng 2019;24:06019003. https://doi.org/10.1061/(ASCE)BE.1943-5592.0001431.

[17] Tohme R, Yarnold M. Steel bridge load rating impacts owing to autonomous truck platoons. Transp Res Rec 2020;2674:57–67. https://doi.org/10.1177/0361198120902435.

[18] Yang D, Kuijpers A, Dane G, der Sande T, van.. Impacts of large-scale truck platooning on Dutch highways. Transp Res Procedia 2019;37:425–32. https://doi.org/10.1016/j.trpro.2018.12.212.

[19] Deng L, Yu Y, Zou Q, Cai CS. State-of-the-art review of dynamic impact factors of highway bridges. J Bridg Eng 2015;20:04014080. https://doi.org/10.1061/(ASCE)BE.1943-5592.0000672.

[20] Brady SP, Gonzalez A, Znidaric A, O'Brien EJ. Impact factors on medium span bridges due to multiple vehicle presence. In: Proceedings of the 7th International Symposium on Heavv Vehicle Weights & Dimensions; 2002 Jun 16–20; Delft, The Netherlands. Delft: Technical University; 2002. p. 1–10.

[21] Brady SP, O'Brien EJ. Effect of vehicle velocity on the dynamic amplification of two vehicles crossing a simply supported bridge. J Bridg Eng 2006;11:250–6. https://doi.org/10.1061/(ASCE)1084-0702(2006)11:2(250).

[22] Zhang N, Tian Y, Xia H. A Train-bridge dynamic interaction analysis method and its experimental validation. Engineering 2016;2:528–36. https://doi.org/10.1016/J.ENG.2016.04.012.

[23] Yang YB, Yau JD, Wu YS. Vehicle-bridge interaction dynamics-with applications to high-speed railways. World Scientific Publishing Co. Pte. Ltd; 2004. https://doi.org/10.1142/9789812567178.

[24] Mao L, Lu Y. Critical speed and resonance criteria of railway bridge response to moving trains. J Bridg Eng 2013;18(2):131–41. https://doi.org/10.1061/(ASCE)BE.1943-5592.0000336.

[25] Xia H, Li HL, Guo WW, De Roeck G. Vibration resonance and cancellation of simply supported bridges under moving train loads. J Eng Mech 2014;140:04014015. https://doi.org/10.1061/(asce)em.1943-7889.0000714.

[26] Ministry of Transport of the People's Republic of China. JTG D60-2015: General specifications for design of highway bridges and culverts. Chinese standard. Beijing: China Communications Press; 2015. Chinese.

[27] LRFDBDS-9: AASHTO LRFD bridge design specifications. American standard. Washington: American Association of State Highway and Transportation Officials (AASHTO); 2020.

[28] Deng L, Cai CS. Development of dynamic impact factor for performance evaluation of existing multi-girder concrete bridges. Eng Struct 2010;32:21–31. https://doi.org/10.1016/j.engstruct.2009.08.013.

[29] Meyer MW, Cantero D, Lenner R. Dynamics of long multi-trailer heavy vehicles crossing short to medium span length bridges. Eng Struct 2021;247:113149. https://doi.org/10.1016/J.ENGSTRUCT.2021.113149.

[30] Deng L, Chen Y, Han W, Wang W. Studying impact factors for short- and medium-span simply supported concrete highway bridges and its suggested values. China J Highw Transp 2020; 33: 69–78. Chinese. https://doi.org/10.19721/j.cnki.1001-7372.2020.01.007.

[31] Xia H, Zhang N, Guo WW. Analysis of resonance mechanism and conditions of train-bridge system. J Sound Vib 2006;297:810–22. https://doi.org/10.1016/j.jsv.2006.04.022.

[32] Cai CS, Shi XM, Araujo M, Chen SR. Effect of approach span condition on vehicle-induced dynamic response of slab-on-girder road bridges. Eng Struct 2007;29:3210–26. https://doi.org/10.1016/j.engstruct.2007.10.004.

[33] Deng L, Cao R, Wang W, Yin X. A multi-point tire model for studying bridge-vehicle coupled vibration. Int J Struct Stab Dyn 2016;16:1–22. https://doi.org/10.1142/S0219455415500479.

[34] Chen SZ, Feng DC, Sun Z. Reliability-based vehicle weight limit determination for urban bridge network subjected to stochastic traffic flow considering vehicle-bridge coupling. Eng Struct 2021;247:113166. https://doi.org/10.1016/j.engstruct.2021.113166.

[35] Deng L, Duan L, He W, Ji W. Study on vehicle model for vehicle-bridge coupling vibration of highway bridges in China. China J Highw Transp 2018;031:92–100. http://zgglxb.chd.edu.cn/EN/Y2018/V31/I7/92.

[36] Harris NKÃ, Obrien EJ, González A, Gonza A. Reduction of bridge dynamic amplification through adjustment of vehicle suspension damping. J Sound Vib 2007;302:471–85. https://doi.org/10.1016/j.jsv.2006.11.020.

[37] The expert committee of Ministry of Transport of China. General design drawing of superstructure series of highway bridge structure. Beijing: China Communications Press; 2010.

[38] Li PF, Wang YF, Liu BD, Su L. Damping properties of highway bridges in China. J Bridg Eng 2014;19(05):04014005. https://doi.org/10.1061/(ASCE)BE.1943-5592.0000578.

[39] Deng L, Cai CS. Bridge model updating using response surface method and genetic algorithm. J Bridg Eng 2010;15(5):553–64. https://doi.org/10.1061/(ASCE)BE.1943-5592.0000092.

[40] Múčka P. Simulated Road Profiles According to ISO 8608 in vibration analysis. J Test Eval 2017;46:20160265. https://doi.org/10.1520/JTE20160265.

[41] ISO. 8608: mechanical vibration—road surface profiles—reporting of measured data. ISO standard. Geneva: International Organization for Standardization (ISO); 2016.

[42] Deng L, Ling TY, He W, Kong X. Refined tire model for analysis of highway vehicle-bridge system vibration. China J Highw Transp 2022;35(4):108–16. https://doi.org/10.19721/j.cnki.1001-7372.2022.04.008 (Chinese).

[43] Eurocode C.E.N. 1 1: actions on structures—part 2: traffic loads on bridges. European standard. European Committee for Standardization; 2003.